



Experimental investigation of tensile properties and microstructure of TIG welded dissimilar joints of Al6061/Al5083 Aluminium alloy

Vijay Verma^{a*}, Aman Singh^a, Arun Kumar Pandey^a, Chaitanya Sharma^b, Pankaj Sonia^c, & Kuldeep Kumar Saxena^c

^aMechanical Engineering Department, Bundelkhand Institute of Engineering and Technology, Jhansi, Uttar Pradesh 284 128, India

^bMechanical Engineering Department, Rustam Ji Institute of Technology, Border Security Force Academy Tekanpur, Madhya Pradesh 475 005, India

^cDepartment of Mechanical Engineering, GLA University Mathura, Uttar Pradesh 281 406, India

Received: 6 February, 2021 ; Accepted: 1 September, 2021

The welding of aluminium alloys especially in dissimilar combination is challenging owing to numerous problems. The present study focuses to optimize processes parameters for dissimilar welding of 6 mm thick dissimilar Al-6061 and Al-5083, using Tungsten Inert Gas welding as well as to investigate the influence of the process parameters on tensile properties and microstructure of developed welds. A single V-butt joint configuration (bevel angle 60° and root gap 2 mm) of plates was used for welding. Three levels of input parameters viz. voltage, current and welding speed were selected for performing experiments as per L9 orthogonal array. The hardness and tensile strength were taken as output parameters or performance characteristic in the study. The optimum parameter settings for highest heat affected zone hardness and ultimate tensile strength of dissimilar welds have been suggested by using S/N ratio. The result predicted by optimization has an error of 2-3%. Finally, the effects of voltage, current and welding speed on micro structure, hardness and tensile strength of welds have been investigated. Welding speed and current were the most influencing process parameter for controlling the hardness of HAZ and tensile strength of the welds.

Keywords: Dissimilar Aluminium Alloy, TIG welding, Tensile properties, Microstructure, Optimization

1 Introduction

Aluminium is an environmental friendly and green material as it can be easily and efficiently be recycled infinitely^{1,2}. Due to its high specific strength, stiffness and good corrosion and oxidation resistance aluminium becomes an important substitute material to most of the engineering materials including steel³. Thus, aluminium fits for vast application in aerospace industries, high speed and light weight vehicles, marine and other engineering sectors for various structural applications^{4,5,6}. For fabrication of complex structures and equipment, fusion welding is mostly used as it is least expensive, fast, easy to use and reliable process^{7,8,9}. Welding of aluminium alloys is not only challenging due to high thermal conductivity, oxide layer formation but also has adverse effect on mechanical properties of welds on account of various defects and metallurgical changes. Porosity, voids, loss of alloying elements, distortion, development of residual stress, hot cracking, localized strength reduction, formation of Heat Affected Zone (HAZ)^{9,10}

are some main problems associated with fusion welding of aluminium alloys. Formation of Al₂O₃ solid inclusion was also reported in literature^{11,12}. These problems become more crucial while performing welding of dissimilar aluminium alloys because of different chemical composition, mechanical and thermal properties^{13,14,15}. The adverse effect of fusion welding on aluminium alloy can be reduced by controlling the heat input which can be governed by process parameter¹⁶. Friction stir welding have some advantages over fusion weld but also have its own characteristic demerits^{17,18,19}. The prediction of weldment strength become more difficult when dissimilar alloys having different melting point and thermal conductivity are to be welded by fusion welding techniques.

There are many studies present in literature on the effect of process parameter on tensile properties and microstructure of welded joints of similar or dissimilar aluminium alloy. Mostly the work was concentrated on parametric study. Still, very few studies were present in literature which explored the optimization of process parameter and investigated their effect on microstructure, hardness, and tensile

*Corresponding author (E-mail: vijay020180@gmail.com)

strength of welded joints of 6061-T6 and 5083-O, dissimilar aluminium alloys welding by tungsten inert gas (TIG) welding. The present work aims to analyse systematically the effect of welding process parameters viz. welding current, voltage, and welding speed on microstructure, hardness and tensile behaviour of TIG welded 6061-T6 and 5083-O dissimilar aluminium alloys.

2 Materials and Methods

TIG welding was performed at M/s Perfect Laser Technology Sector-9 Noida, India, on ECCKO (315 P) TIG welding machine. ER 4043 was used as filler material for TIG welding. The Inert gas, Argon was used as shielding gas to avoid atmospheric contamination of weld pool during welding. For welding, the strip of both the base metals of size 300 mm × 50 mm × 6 mm was obtained by machining. The edge of the plates to be welded had 60° V groove, 2 mm root face and 1mm root opening. Before welding, the edges of the plates were cleaned by acetone to remove oxide layer, grease, foreign particles, and other impurities present on them. During welding, welding torch was kept slightly close to the edge of Al-6061 alloy²⁰. Photograph of one such TIG welded joint of 6061-T6 and 5083-O dissimilar aluminium alloys is shown in Fig. 1. The weld bead seems to be uniform, smooth, and free from defect like spatter, under cut etc. The penetration was also complete.

Initially the visual inspection was carried out on the welded joints to identify defects present, if any and segregate them. After visual inspection the specimen for tensile testing, hardness testing and micro structural analysis was machined by wire cut Electric Discharge Machine (EDM) from the welded plates so that welding direction was perpendicular to that of loading direction. Tensile tests specimens were machined as per ASTM B557 M (derived from ASTM-E 08M) standard²¹ and shown in Fig. 2. The tensile tests were conducted on computerized universal testing machine (UTM) (25 kN, Nano Plug

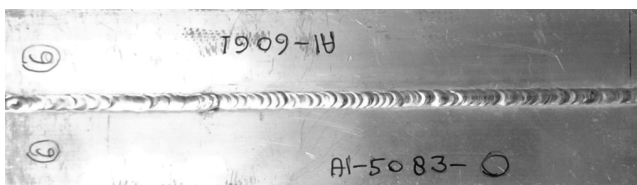


Fig. 1 — Dissimilar TIG weldjoint of Al6061-T6, and Al5083-O aluminium alloys.

and play BISS, India). The hardness along the transverse section of the welded joints was measured at mid transverse plane after polishing, using Vickers hardness testing machine (VM-50, Fuel Instruments Ltd, India). A load of 5 Kg was used with a dwell time of 30 sec for hardness indentation. Optical microscope (DMIL M LED, Leica) was used for microstructural analysis while scanning electron microscope (Carl Zeiss EVO-50 at IIT Kanpur) was utilized studying fracture surface of tensile test specimens. The polished samples were etched with Keller’s (190 ml refine water + 5 ml HNO₃+ 3 ml HCL+ 2 ml HF) solution for 60 seconds²².

Based on the literature and pilot experiments, the different process parameters such as welding current (A), voltage (V) and welding speed (WS) have been selected as input process parameters, while gas flow rate of 10 l/min was taken as constant. For conducting the experiments, a well-designed L₉ Orthogonal Array (OA) has been used. This OA has been selected based on the number of process parameters, their levels and the total degree of freedom. Three levels of the three input control parameters used in this work are shown in Table 1.

The experiments have been conducted by using the values of different process parameters corresponding to the L₉ OA. For each experiment, the corresponding hardness in different regions of developed welds i.e., 5083 base metal, 5083 HAZ (HAZ-I), weld pool, 6061 HAZ (HAZ-II) and 6061 base metal have been measured. All the measured values of hardness are shown in Table 2. Tensile tests on the welded specimen have also been conducted and the measured values (mean of three repeated testing) of ultimate tensile strength are also shown in Table 2.

2.1 Optimization

The optimization of hardness and ultimate tensile strength of dissimilar welds has been carried out by



Fig. 2 — Tensile test specimen.

Table 1 — Input parameters

Parameters	Levels	Symbol	-1	0	+1
Voltage (V)		A	22	24	26
Current (A)		B	162	164	166
Welding Speed (mm/min)		C	157	162	167

Table 2 — Input control parameter taken and response

Sample No.	Voltage (V)	Current (A)	Welding Speed (mm/min)	Vickers Hardness (HV)					Ultimate Tensile Strength (MPa)
				Base Metal 5083	HAZ 5083 (HAZ-I)	Weld Metal	HAZ 6061 (HAZ-II)	Base Metal 6061	
1	22	162	157	93.9	89.5	49.8	74.8	96.6	68.94
2	22	164	162	93.9	90.8	41.2	70.3	96.6	142.71
3	22	166	167	93.9	90.3	50.02	79.9	96.6	120.25
4	24	162	162	93.9	91.2	51	68.8	96.6	119.00
5	24	164	167	93.9	90.1	54.2	70.2	96.6	116.96
6	24	166	157	93.9	89.8	54.8	74.5	96.6	157.83
7	26	162	167	93.9	90.3	48.3	75.5	96.6	116.96
8	26	164	157	93.9	89.6	52	63.8	96.6	159.83
9	26	166	162	93.9	91.5	59.7	73.3	96.6	167.13

Table 3 — S/N Ratio for different responses

Sample No.	Voltage (V)	Current (A)	Welding Speed (mm/min)	S/N Ratio Hardness (HAZ-I)	S/N Ratio Hardness (HAZ-II)	S/N Ratio Ultimate Tensile Strength
1	22	162	157	-39.0365	-37.4780	27.22322
2	22	164	162	-39.1617	-36.9391	37.06788
3	22	166	167	-39.1138	-38.0509	35.58038
4	24	162	162	-39.1999	-36.7518	35.49034
5	24	164	167	-39.0945	-36.9267	35.33866
6	24	166	157	-39.0655	-37.4431	37.94264
7	26	162	167	-39.1138	-37.5589	35.33866
8	26	164	157	-39.0462	-36.0964	38.05202
9	26	166	162	-39.2284	-37.3021	38.43997

using Taguchi Methodology. Signal-to-noise ratio is a measure used in science and engineering that compares the level of a desired signal to the level of background noise. For the optimization, the signal to noise (S/N) ratios for all the quality characteristics have been calculated by using lower the better and higher the better depending upon the requirements^{23,24,25,26}. The calculated values of S/N ratio for all three input parameters have been shown in Table 3. For HAZ, the S/N ratio is calculated by using smaller the better type while for the ultimate tensile strength, it is larger the better type.

The main effect plot of the effect of input parameters on the output responses considered in this study are presented in Fig. 3. From the Fig. 3, voltage was found major influential parameter for controlling the hardness and UTS of the welded joint. On 5083 side the increase in voltage has a good effect as the hardness of the HAZ-I decreases with increase in voltage. The increase in voltage has a reverse effect on 6061 side hardness. Such behaviour may be due to different thermal conductivity, weld thermal cycle and resulting microstructure. Higher thermal conductivity allows fast conduction of weld heat to larger area surrounding the weld pool which in turn results in

larger size HAZ and difficult to normalize the ill effect of random heat source.

ANOVA is statistical technique to obtain variance of the data. The result data of hardness (HAZ-I and II) and ultimate tensile strength was analysed using MINITAB software. The ANOVA table for HAZ-I, HAZ-II and UTS of Al6061/Al5083 welds is shown in Table 4 (a-c) respectively. ANOVA method is applied to observe percentage of contribution.

The contributions of different process parameters on hardness (HAZ-I and HAZ-II), and ultimate tensile strength have been analysed and shown in Fig. 4. The analysis showed that welding speed has maximum contribution (91.99%) on the hardness of HAZ-I while the effects of other parameters may be neglected as their contribution is very less. For the hardness of HAZ-II, welding current showed the maximum contribution (49.24) followed by the welding speed (27.69%) and voltage (22.57%). The effect of error on hardness in both the HAZs is very less almost less than 0.5%. While for the ultimate tensile strength, welding current showed the maximum contribution (41.94%) followed by the voltage (30.66%) and welding speed 26.88%. From this analysis it can be concluded that welding speed

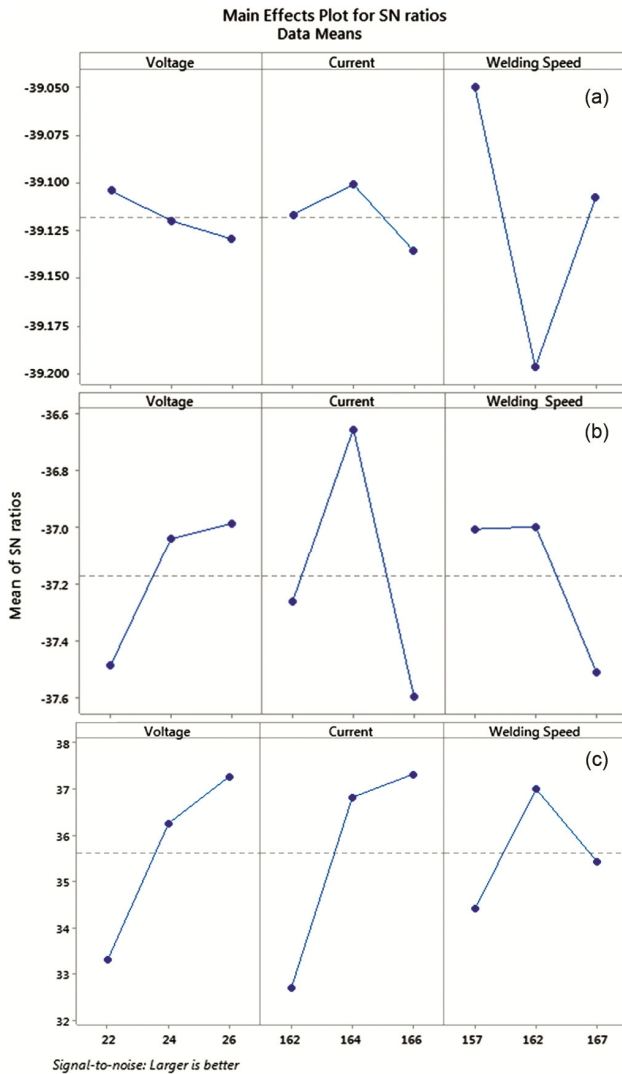


Fig. 3 — Main effect plot for (a) HAZ-I, (b) HAZ-II, and (c) UTS of Al6061/Al5083welds.

and welding current are the more effective parameters as compared to the voltage for all responses.

With the help of the S/N ratio, the response tables have been generated by using MINITAB software and are shown in Table 5 (a-c). The response table for HAZ-I, HAZ-II and ultimate tensile strength is shown in Table 5(a-c) respectively. The first rank was given to the current as per delta values for all responses because it is the most important parameter among the all three input parameters used for TIG welding of dissimilar Al-alloys. The response tables can be used to obtain optimum process parameters. The optimum process parameters will be that level of process parameters which corresponds to the maximum values of responses ^[27].

By using the above concept, the optimum process parameters for all three responses have been found and these are shown in Table 6. The optimum parameter setting for minimum hardness at HAZ-I may be found at third level of A (voltage), second level of B (welding current) and third level of C (welding speed) i.e. $A_3B_2C_3$. Similarly for the minimum hardness at HAZ-II may be found at $A_3B_2C_1$ while the optimum values of ultimate tensile strength may be observed at $A_3B_3C_2$ ²⁸. The numerical values of different process parameters for getting the optimum responses are given in Table 6. For example, the optimum values of ultimate tensile strength may be found at Voltage-26 V, Current-166 Amp and Welding Speed-162 mm/min.

3 Results and Discussion

The control parameters along with the responses are shown in Table 2. From this table, the hardness in different zones and tensile strength increases with increase in welding current and voltage. Increase in welding speed beyond the moderate value may decrease the hardness and tensile properties. The increase in tensile strength with increase in welding voltage and current may be due to increase depth of penetration and increase fusion of base metal with the filler. The higher current and voltage during welding at constant speed will increase the heat input in the joint thus able to melt more metal. This increase in heat input will also increase the HAZ zone which is a characteristic defect of fusion welding.

Figure 5 shows the macroscopic images of the cross section of welded joints developed using various combination of process parameters. From the images we can observe that the macrostructure of welded joints was affected by the process parameters. Welded joints 2, 3, and 4 showed incomplete fusion of edges and penetration whereas bead profile was improper for welded joints 4, 5, and 8. Undercut can be observed on welded joint 5 and 6. Significant distortion can also be clearly observed for welded joint 8. Spatter, voids and porosity was not observed in formed welded joints.

Microstructure of welded joint 9 (voltage 26 V, current 166 A and welding speed 162 mm/min) which yielded maximum weld properties is presented in Fig. 6(a), letter B-E in macrograph shows the location of zone from where microstructure was obtained. The microstructure of the HAZ zones of both Al5083 and Al6061 and the weld pool metal i.e., fusion zone was

Table 4 (a) — ANOVA for HAZ –I (Al5083-O)

Source	DF	Seq SS	Contribution	Adj SS	Adj MS	F-Value	P-Value
Voltage	2	0.000000	2.71%	0.000000	0.000000	14.46	0.065
Current	2	0.000000	5.11%	0.000000	0.000000	27.21	0.035
Welding Speed	2	0.000000	91.99%	0.000000	0.000000	490.28	0.002
Error	2	0.000000	0.19%	0.000000	0.000000		
Total	8	0.000000	100.00%				

Table 4 (b) — ANOVA for HAZ –II (Al6061-T6)

Source	DF	Seq SS	Contribution	Adj SS	Adj MS	F-Value	P-Value
Voltage	2	46.285	22.57%	46.285	23.1423	44.73	0.022
Current	2	100.961	49.24%	100.961	50.4806	97.58	0.010
Welding Speed	2	56.773	27.69%	56.773	28.3866	54.87	0.018
Error	2	1.035	0.50%	1.035	0.5173		
Total	8	205.054	100.00%				

Table 4 (c) — ANOVA for UTS of Al6061/Al5083 welds

Source	DF	Seq SS	Contribution	Adj SS	Adj MS	F-Value	P-Value
Voltage	2	1616.45	30.66%	1616.45	808.23	58.98	0.017
Current	2	2210.83	41.94%	2210.83	1105.41	80.67	0.012
Welding Speed	2	1417.26	26.88%	1417.26	708.63	51.71	0.019
Error	2	27.41	0.52%	27.41	13.70		
Total	8	5271.95	100.00%				

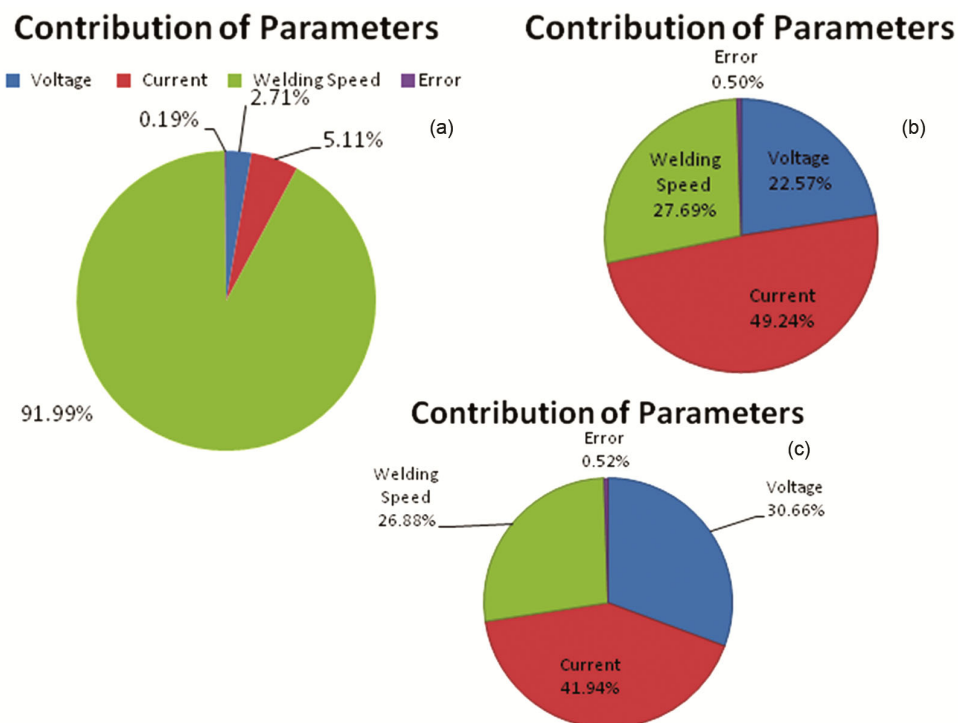


Fig. 4 — Contribution of parameters (a) hardness at HAZ-I, (b) hardness at HAZ-II, and (c) ultimate tensile strength of Al6061/Al5083 welds

clearly visible in the images of Fig. 6. Partially melted region (Fig. 6 (b)), fusion zone (Fig. 6(c)) and heat affected zone (Fig. 6(d and e)) showed different grain structure. Formation of grains began at partially

melted grain which acted as readymade nuclei for grain formation and grew in the direction of maximum cooling rate. The grains were equiaxed in close vicinity of fusion boundary. Later, on the cast

columnar dendritic grains can be seen in fusion zone, grown toward the centre of weld pool. Compared to fusion zone, both the heat affected zone showed equiaxed grain structure. Heat affected zone on Al6061 (Fig. 6 (e)) side had coarser equiaxed grains

than Al5083 side (Fig. 6 (d)) probably due to more post weld grain growth. This evolution of microstructure is due to weld thermal cycle observed during fusion of base metal with weld metal ^{4, 29}. No void or a crack was observed in fusion zone.

Figure 7 shows the variation of Vickers hardness in different zones of welds taken progressively from weld centre towards the end at mid plane. Welding decreased the hardness in the fusion zone which then increased on moving towards the base metal i.e., from the centre toward the ends of weld joint. The minimum hardness was in the fusion zone. The decrease in hardness in heat affected zone was found to be more in case of Al6061 than Al 5083. The

Table 5 (a) — Response table for hardness HAZ-I

Level	Voltage	Current	Welding Speed
1	-39.10	-39.12	-39.05*
2	-39.12	-39.10*	-39.20
3	-39.13	-39.14	-39.11*
Delta	0.03	0.04	0.15
Rank	3	2	1

Table 5 (b) — Response table for hardness HAZ-II

Level	Voltage	Current	Welding Speed
1	-37.49	-37.26	-37.01*
2	-37.04	-36.65*	-37.00
3	-36.99*	-37.60	-37.51
Delta	0.50	0.94	0.51
Rank	3	1	2

Table 5 (c) — Responsetable for ultimate tensile strength

Level	Voltage	Current	Welding Speed
1	33.29	32.68	34.41*
2	36.26	36.82	37.00*
3	37.28	37.32*	35.42
Delta	3.99	4.64	2.59
Rank	2	1	3

Table 6 — Optimum Process Parameters for different Responses

Responses	Optimal parameter	Numerical values of process parameters
Hardness (HAZ 1)	A ₃ B ₂ C ₃	Voltage-26 V, Current-164 Amp and Welding Speed-167 mm/min
Hardness (HAZ 2)	A ₃ B ₂ C ₁	Voltage-26 V, Current-164 Amp and Welding Speed-157 mm/min
Tensile strength	A ₃ B ₃ C ₂	Voltage-26 V, Current-166 Amp and Welding Speed-162 mm/min

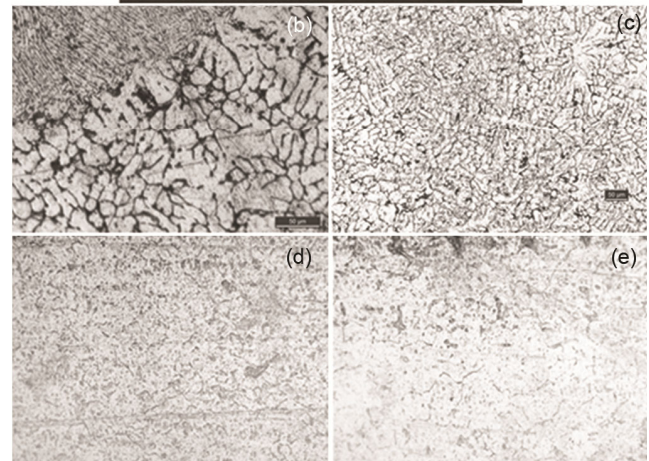
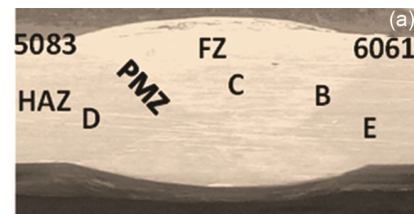


Fig. 6 — Microstructure of b) PMZ, c) FZ, d) Al5083 HAZ, and e) Al6061 HAZ of TIG Weld.



Fig. 5 — Macroscopic images of weld cross section.

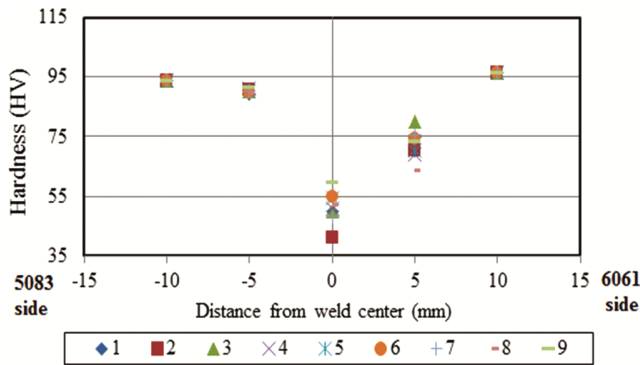


Fig. 7 — Hardness profile of weld joints fabricated using different welding condition

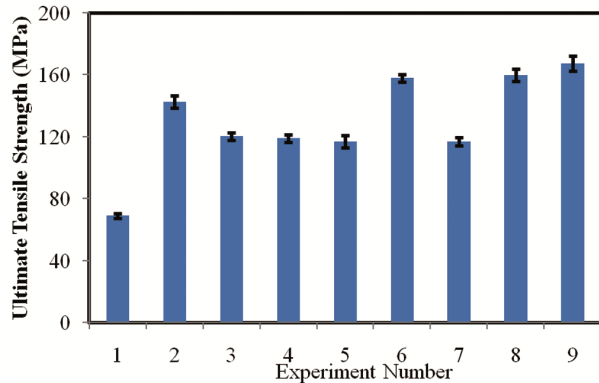


Fig. 8 — Ultimate tensile strength of welded specimen

hardness in heat affected zone was found to be less than respective base metal. The decrease in hardness in fusion zone is due to dissolution of strengthening precipitate, loss of alloying elements and formation of cast dendritic grain structure. It is clear that dissolution was dominant than re-precipitation of strengthening precipitates which could not restore the fusion zone hardness to initial level because of significant softening. Another reason for lower fusion zone hardness is low hardness of ER 4043 filler than both the base materials. Moreover, ER 4043 is prone to micro porosity during solidification after welding than other filler used and may be another reason of decrease fusion zone hardness. Similar results have reported hardness of less than 40 Hv in fusion zone in case of welding of AA6061 with ER 4043 filler³⁰. In case of Al6061, low HAZ hardness can be attributed to coarsening of strengthening precipitates and grains whereas for Al5083 HAZ, loss of hardness was insignificant may be due to grain coarsening as base metal was welded in annealed O temper which cannot be softened further by welding at the cost of hardening effect^{31,32,33}.

The variation of tensile strength of the TIG welded joint of Al 6061 and Al5083 alloy is shown in Fig. 8. The strength of welded joint increased with increase in welding current and voltage. The moderate increase in welding speed also increases the tensile strength of the joint. Increase in heating rate at lower welding torch travel speed and proper fusion of base metal and filler metal in liquid condition may resulted in higher tensile strength of the joint. On further increase in welding speed the tensile strength decreased. The decrease in tensile strength may be due to lesser heat input resulting in improper fusion. Non optimal combination of parameters may cause larger HAZ, porosity, voids and other defects in more numbers which support the decrease in tensile strength and hardness of the welded joints. The re-precipitation of strengthening precipitates in the fusion zone may be the other reason for increase in tensile strength of the welded joint. The more percentage of Mg₂Si precipitates higher will be the tensile strength of the specimen^{17,32}.

In all cases the fracture occurred in the weld bead of weld joint which showed lowest hardness. Generally, in case of dissimilar metal welded joint the fracture of tensile specimen was reported to be in weak metal, especially in or near the HAZ zone^{17,18}. Similarly, failure of weld was observed from base metal or weld region (stir zone) involving base metal in O temper or T6 temper^[34].

Figure 9 (a and c) shows the SEM image of the fracture surfaces of tensile tested specimen of test condition set (1) and (9). Tensile strength of test condition of set number (1) result in minimum tensile strength while tensile test of test condition (9) results in maximum tensile strength. As expected, the fracture surface was rough and fibrous as in case of fracture of ductile material. Dimples were formed on the fracture surface of both the specimen. The size of dimples formed on the fracture surface of test specimen number (9) are closely spaced and more in number compared to the number of dimples formed on the fracture surface of specimen (1). Some deep holes were also observed on the SEM images. These deep holes may be formed due to voids formed during welding. The number of voids present on fracture surface of specimen (1) was quite more and has higher depth (Fig. 9(b)) compared to the voids present on the fracture surface of sample (9) (Fig. ((d)). The increase in number of voids and size of voids suggest lower tensile strength of the welded joint.

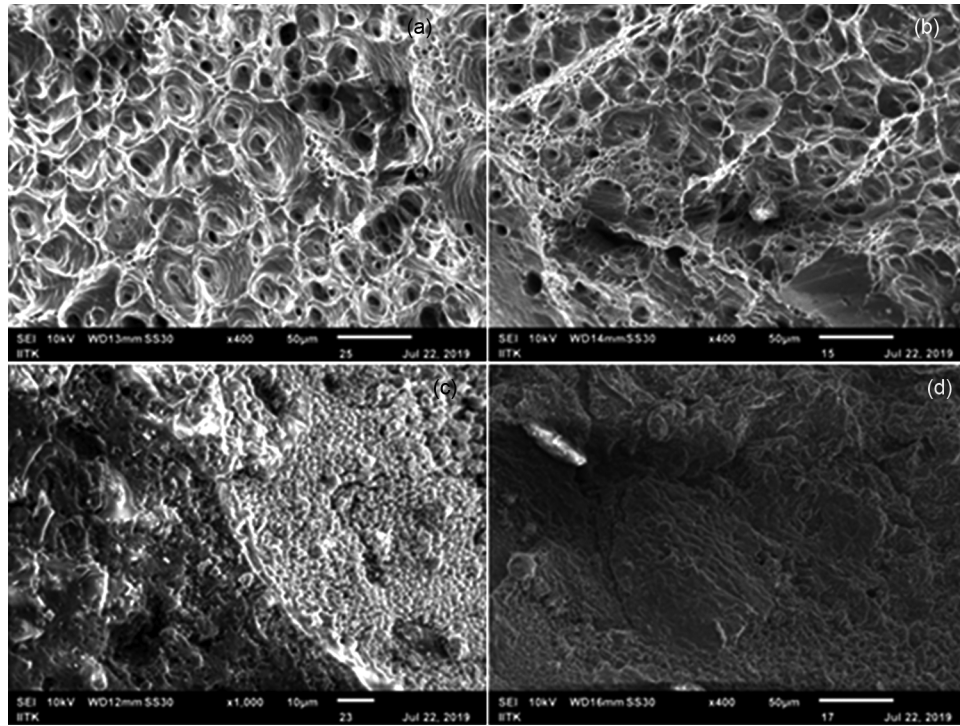


Fig. 9 — Fracture surface of weld joints (a) & (b) experiment no. 1, (c) experiment no. 9, and (d) high magnification.

4 Conclusion

Aluminium alloy Al 6061 and Al5083 was successfully welded by using tungsten inert gas arc welding (TIG) with ER4043 filler to optimize the input parameters and study their effect on hardness, tensile strength, and microstructure of Al6061/Al5083 welds. Following are the major outcomes of this study:

- Input process parameters for TIG welding of dissimilar aluminium alloy Al6061 and Al 5083 with ER4043 as filler material can be optimized using L₉ Orthogonal Array and Taguchi technique.
- Welding speed and welding current had maximum contribution (91.99%) on HAZ-I (Al5083), and (49.24%) HAZ-II (Al6061) hardness whereas welding current showed maximum contribution (41.94%) on weld ultimate tensile strength.
- The optimum combination of input parameters was voltage 26 V, current 166 A, and welding speed of 162 mm/min which yielded maximum ultimate tensile strength of 167.13 MPa and hardness of 91.5 HV, 73.3 Hv and 59.7 Hv for HAZ-I, HAZ-II and fusion zone respectively.
- Non optimal combination of parameters may cause larger HAZ, porosity, voids, and other defects in more numbers as well greater is the

extent of softening and coarsening resulting in low tensile strength and hardness of welds.

- The fracture of all the welds occurred from lowest hardness fusion zone during tensile test where dissolution dominated reprecipitation. Mode of failure was ductile as fractured surface were covered with dimples.

Acknowledgement

The authors thanks Dr. D.K. Shukla, Department of Mechanical Engineering, MNNIT, Allahabad for helping in conducting the tensile testing. Authors also thanks MPS department of IIT Kanpur for scanning electron microscopy of fractured surface of tensile specimens.

References

- 1 Buchta A M, Kiesswetter B E, Schaper B M, Zschiesche C W, Schaller D K H, Kuhlmann A A, & Letzel A S, *Environ Toxicol Pharmacol*, 19(3) (2005) 677.
- 2 Ibrahim A I, Zamzami, & Susmel L, *Int J Fatigue*, 101(2) (2017) 137.
- 3 Heinena P, Wub H, Olowinskya A, & Gillnera A, *Phys Procedia*, 56 (2014) 554.
- 4 Sharma S K, Patel P, Chandra, M Rajak A, & Sharma C *J Inst Eng India Ser D* (2022). <https://doi.org/10.1007/s40033-021-00324-8>
- 5 Milani M A, Paidar M, Khodabandeh A, & Nategh S, *Int J Adv Manuf*, 82 (2016)1495.

- 6 Sharma C, Dwivedi D K, & Kumar P, *Proce Eng*, 64 (2013) 1384.
- 7 Koushki A R, Goodarzi M, & Paidar M, *Int J Miner Metall Mater*, 23 (2016) 1416.
- 8 Khan N U, Rajput S K, Gupta V, Verma V, & Soota T, *Mater Today Proc*, 18 (2019) 2550.
- 9 Menzemer C C, Hilty E, Morrison S M, & Srivatsan R T S, *Metals*, 6 (2016) 52.
- 10 Woelke P B, Hiriyur B K, Nahshon K, & Hutchinson J W, *Eng Fract Mech*, 175 (2017) 72.
- 11 Jeong H, Park K, Baek B, & Cho J, *Int J Heat Mass Transfer*, 138 (2019) 729.
- 12 Mercan E, Ayan Y, & Kahraman N, *Int J Eng Sci Tech*, 23(4) (2020) 723.
- 13 Baghel P K, & Nagesh D S, *Indian J Eng Mater Sci*, 25 (2018) 147.
- 14 Vijay S, Rajanarayanan S, & Ganeshan G N, *Mater Today Proc*, 21(1) (2020) 384.
- 15 Nguyen V N, Nguyen Q M, & Huang S C, *Materials*, 11 (2018) 1136.
- 16 Balasubramanian M, Jayabalan V, & Balasubramanian V, *Int J Adv Manuf Syst*, 35 (9) (2008) 852.
- 17 Sharma V, Sharma C, Upadhyay V, & Singh S, *Mater Today Proc*, 4(2) (2017) 628.
- 18 Sharma C, Tripathi A, Upadhyay V, Verma V, & Sharma S K, *J Eng Res*, (2021) 1. <https://doi.org/10.36909/ jer.ICCEM ME.15693>.
- 19 Sharma C, Tripathi A, Upadhyay V, Verma V, & Sharma S K, *J Inst Eng (India): D*, 102 (2) (2021) 549.
- 20 Verma R P, Pandey K N, & Sharma Y, *Proc Inst Mech Eng B J Eng Manuf*, (2014)1.
- 21 ASTM B557-15, West Conshohocken, PA, 2015.
- 22 Verma V, Patel S, Swarnkar V, & Rajput S K, *Mater Today Proc*, 18 (2019) 2374.
- 23 Shrivastava P K, Singh B, Shrivastava Y, & Pandey A K, *J Braz Soc Mech Sci Eng*, 41, 216, (2019) 1.
- 24 Verma V, & Sajeevan R, *Mater Today Proc*, 2 (4-5) (2015) 2581.
- 25 Verma V, & Sahu R, *Mater Today Proc*, 4 (2) (2017)1893.
- 26 Verma V, Kumar J, & Singh A, *Mater Today Proc*, 25 (2020) 793.
- 27 Singh T, & Pandey A K, *Rec Adv Mech Eng*, (2021) 343.
- 28 Shrivastava P K, & Pandey A K, *Phys Technol*, 89 (2018) 369.
- 29 Sharma C, Upadhyay V, & Tripathi A, *Int J Mech Mechatron Eng*, 9 (12)(2015) 2051.
- 30 Che Lah N A, Ahmad I M F, Jalar A, Sharif J, Othman N K, & Rashdi N M, *Adv Mater Res*, 146(2011)987.
- 31 Sato Y S, Kokawa H, & Enomoto M, *Metall Mater Trans*, 30(1999) 2429.
- 32 Sharma C, Dwivedi D K, & Kumar P, In: Suarez CE (eds) *Light Metals*, (2012), 503, Cham. https://doi.org/10.1007/978-3-319-48179-1_85.
- 33 Jaiswal S, Verma V, & Sharma C, *Lect Notes Mech Eng*, 2021. doi.org/10.1007/978-981-15-8704-7.
- 34 Kumar R, Upadhyay V, & Sharma C. *Indian J Eng Mater Sci*, 28 (2021) 574.